Measurement 46 (2013) 1572–1584

Contents lists available at SciVerse ScienceDirect

Measurement

journal homepage: www.elsevier.com/locate/measurement

Effect of work material hardness and cutting parameters on performance of coated carbide tool when turning hardened steel: An optimization approach

Satish Chinchanikar *, S.K. Choudhury

Mechanical Engineering Department, Indian Institute of Technology, Kanpur 208 016, India

ARTICLE INFO

Article history:
Received 9 July 2012
Received in revised form 9 November 2012
Accepted 26 November 2012
Available online 13 December 2012

Keywords:
Cutting force
Surface roughness
Tool life
Hardened steel
Coated carbide tool
Analysis of Variance (ANOVA)

ABSTRACT

In present work performance of coated carbide tool was investigated considering the effect of work material hardness and cutting parameters during turning of hardened AISI 4340 steel at different levels of hardness. The correlations between the cutting parameters and performance measures like cutting forces, surface roughness and tool life, were established by multiple linear regression models. The correlation coefficients found close to 0.9, showed that the developed models are reliable and could be used effectively for predicting the responses within the domain of the cutting parameters. Highly significant parameters were determined by performing an Analysis of Variance (ANOVA). Experimental observations show that higher cutting forces are required for machining harder work material. These cutting forces get affected mostly by depth of cut followed by feed. Cutting speed, feed and depth of cut having an interaction effect on surface roughness. Cutting speed followed by depth of cut become the most influencing factors on tool life; especially in case of harder workpiece. Optimum cutting conditions are determined using response surface methodology (RSM) and the desirability function approach. It was found that, the use of lower feed value, lower depth of cut and by limiting the cutting speed to 235 and 144 m/min; while turning 35 and 45 HRC work material, respectively, ensures minimum cutting forces, surface roughness and better tool life.

1. Introduction

The machining of hardened steels using polycrystalline cubic boron nitride (PCBN) and ceramic tools is widely accepted as a best replacement to costly grinding operations. However, development in the cemented carbide grades, coating materials and coating deposition technologies have attracted many researchers in the field of hardened steel machining using coated carbide tools.

Lima et al. [1] evaluated the performance of coated carbide inserts. Cutting forces, tool life, and wear mechanisms were assessed during turning of hardened AISI 4340 steel at different levels of hardness 23, 35, 42 and 50 HRC, respectively. Their study concluded that coated carbide tools were unable to work at 50 HRC even at light metal removal rates. Asilturk et al. [2] optimized cutting parameters based on Taguchi method to minimize surface roughness during turning of hardened AISI 4140 steel (51 HRC) with coated carbide tools. The results showed a significant effect of feed rate on the surface roughness.

Suresh et al. [3] evaluated the performance of multilayer CVD coated TiN/TiCN/Al_2O_3 cemented carbide inserts during machining of hardened AISI 4340 steel having hardness of 48 HRC. The analysis of results concluded that, low feed rate and depth of cut and high cutting speed was beneficial for minimizing the machining force and surface roughness. In another study, they observed reduced tool wear with lower cutting speed and lower feed rate [4]. However, selection of the cutting parameters which can

* Corresponding author.
E-mail address: Satish@iitk.ac.in (S. Chinchanikar).

0263-2241/$ - see front matter © 2012 Elsevier Ltd. All rights reserved.
http://dx.doi.org/10.1016/j.measurement.2012.11.032

minimize the surface roughness, cutting forces and produces better tool life is a key issue, which was not considered in their studies. Yusuf and Motorcu [5] developed the surface roughness model in terms of the cutting parameters for turning with TiN-coated carbide tools. The first and second-order models were developed using the experimental data. They observed feed rate as the main influencing factor on the surface roughness.

Noordin et al. [6] investigated the effects of cutting speed, feed and side cutting edge angle of the cutting edge, on cutting force and surface roughness, while machining with coated carbide tools. They observed feed as the most significant factor, which influenced the surface roughness and tangential force, during turning of AISI 1045 steel. Sahoo and Sahoo [7] investigated flank wear, surface roughness, chip morphology and cutting forces in hard turning of AISI 4340 steel (47 HRC); using uncoated and multilayer TiN and ZrCN coated carbide inserts. Experimental results showed that multilayer TiN/TiCN/Al_2O_3/TiN coated carbide inserts performed better than the uncoated and TiN/TiCN/Al_2O_3/ZrCN coated carbide inserts.

In another study, Sahoo and Sahoo [8] developed a mathematical model for surface roughness in turning of high chromium cold worked tool steel (22 HRC). The ANOVA results showed that the feed was the most significant parameter on surface roughness followed by depth of cut and cutting speed. Cakir et al. [9] investigated the effects of cutting parameters and influence of different coating layers on surface roughness during turning of AISI P20 tool steel having hardness 52–55 HRC. A linear, second order (quadratic) and exponential models of surface roughness were developed and found second order model as most appropriate to predict the surface roughness.

Aouici et al. [10] investigated the effects of cutting speed, feed rate, workpiece hardness and depth of cut on surface roughness and cutting force components in hard turning. AISI H11 steel, hardened to 40, 45 and 50 HRC, respectively, was machined using cubic boron nitride tools. Mathematical models were developed for surface roughness and cutting force components using the response surface methodology (RSM). Results showed that the cutting force components were influenced principally by depth of cut and workpiece hardness; however, both feed rate and workpiece hardness had statistical significance on surface roughness.

Lima et al. [11] investigated the machinability of AISI D2 cold work tool steel (50 HRC) and AISI 4340 steel (42 HRC) using ceramic and coated carbide inserts. They observed principal wear mechanism as abrasion and diffusion while machining 42 and 50 HRC steel, respectively. Ozel et al. [12] investigated the surface roughness and cutting forces in hard turning of AISI H13 steel. Significant effect by workpiece hardness, cutting edge geometry, feed rate and cutting speed was observed on surface roughness. Federico et al. [13] performed turning of hardened steel using TiCN/Al_2O_3/TiN coated carbide and PCBN tools, respectively. The results concluded that machining of medium hardened steels was productive with TiCN/Al_2O_3/TiN coated carbide tools.

Mandal et al. [14] assessed the machinability of AISI 4340 steel using Zirconia Toughened Alumina (ZTA) ceramic inserts. Study of analysis concluded that depth of cut followed by cutting speed had a maximum contribution on flank wear. However, feed had a nominal contribution. Neseli et al. [15] investigated the influence of tool geometry on surface finish during turning of AISI 1040 steel. Tool nose radius observed as a dominant factor on the surface roughness. Response surface methodology used to optimize the tool geometry combination in turning.

In the present context of sustainable manufacturing, machining of medium hardened steels with coated carbide tools have become an economical alternative to costly CBN and ceramic tool materials. However, machining of harder workpiece puts some restrictions on cutting conditions so as to have the better tool life, dimensional accuracy and surface finish. Therefore, development of the reliable model which can predict and optimize the performance of coated carbide tools in hardened steel machining will be extremely valuable and represents a key issue.

Although, optimization study and predictive models are available in turning of hardened steel alloys, but studies are mostly performed using CBN or ceramic tools. Moreover, tool life, being an important factor was not considered while optimizing the cutting conditions for surface roughness and cutting forces. Hence, in the present work, performance of coated carbide tool; in terms of cutting forces, surface roughness and tool life is investigated considering the effect of work material hardness and cutting parameters during turning of hardened AISI 4340 steel. Further, correlations between the cutting parameters and the performance measures are established using multiple linear regression models. Adequacy of the developed models is checked using Analysis of Variance (ANOVA) technique. Finally, optimum cutting condition which gives better tool life, minimum surface roughness and cutting forces is suggested for two different levels of work material hardness.

2. Experimental details

2.1. Workpiece materials

AISI 4340 steel having two distinct levels of hardness: 35 (33–35) and 45 (45–47) HRC was used as a workpiece material having diameter of 90 mm. This material is known for properties like high tensile strength, shock resistance, good ductility and wear resistance. It finds application in heavy vehicle crank shafts, connecting rods, gear shafts, cam shafts, spindles, etc. The chemical composition of the workpiece material is given in Table 1.

2.2. Cutting inserts

Experiments were performed using commercially available coated tungsten based cemented carbide inserts. The

Table 1
The chemical composition of AISI 4340 steel by weight percentage.

C	Mn	Si	S	P	Cr	Mo	Ni
0.4	0.65	0.21	0.012	0.015	1.05	0.3	1.36

grade of the inserts is Kennametal KC9110 (CVD with TiCN/Al_2O_3/TiN coating layer sequence) is an ISO class P10 grade with three main layers and several more sub-layers of coating with a total thickness of 18-microns. The main coating layers include: medium temperature titanium carbonitride (TiCN), fine-grain alpha structure aluminum oxide (Al_2O_3), and a thin layer of titanium carbonitride (TiCN) and titanium nitride (TiN). The insets have identical geometry designated by ISO as CNMG 120408 (80° diamond shape with 0.8 mm nose radius). For each experiment a fresh cutting edge was used. A right hand style tool holder designated by ISO as PCBNR 2020K12 was used for mounting the inserts.

2.3. Design of Experiments (DOEs)

Experiments were carried out varying the cutting speed, feed and depth of cut. A premature tool failure was occurred when turning 45 HRC work material at higher cutting speed (>200 m/min). However, no such premature failure was observed when turning 35 HRC work material, even as cutting speed exceeded above 300 m/min. Therefore, two different ranges of cutting speed were selected for different levels of hardness. Ranges of feed and depth of cut were decided on the basis of machine capability, literature review and tool manufacturer's recommendation [16]. The selected ranges of parameters are given in Table 2.

Central rotatable composite design (CCD) test matrix with an alpha value of 1.68179 was used for planning of cutting force and surface roughness experiments [17]. Each numeric parameter was varied over five levels: plus and minus alpha (axial points), plus and minus 1 (factorial points) and the center point. In present work, 20 experiments were performed on each work material to develop a cutting force and surface roughness models.

Tool life experiments were performed based on a CCD test matrix with an alpha value of 1.414. The highest and lowest values of cutting speed and feed are selected as shown in Table 2. A depth of cut was used as 0.8 mm. Additional experiments at various depths of cut were performed to consider the effect of depth of cut on tool life. Uncertainty characterization was not offered in tool life experiments due to the size of the experimental data set.

3. Performing experiments as per DOE

Cutting tests were carried out on a HMT centre lathe with step variable spindle speed and feed under dry cutting conditions. During experiments, tool height, its overhang and tool geometry were kept constant. In turning operations, it is convenient to consider the tool forces as a three-component system as shown in Fig. 1a. These are the tangential component P_1, the feed component P_2 and a radial component P_3.

Table 2
Highest and lowest values of cutting parameters.

Parameter	Lowest	Center point	Highest
Cutting speed [V] (m/min)			
At work material hardness of 35 HRC	100	200	300
At work material hardness of 45 HRC	100	150	200
Feed [f] (mm/rev)	0.1	0.2	0.3
Depth of cut [d] (mm)	0.5	1.5	2.5

3.1. Measuring instruments

Average values of the cutting force components were measured by using a three-component piezo-electric dynamometer (KISTLER Type 9257A) mounted on the cross slide of the lathe (Fig. 1a). A piezoelectric dynamometer consists of stacks of piezoelectric crystals, produces an electric charge which varies in direct proportion with the load acting on the sensor. The dynamometer consists of three-component force sensors; sensitive to pressure in the z direction and the other two responding to shear in the x and y directions, respectively. The generated charge is then converted to a voltage by a charge amplifier. A fast and accurate novel method for time-varying frequency estimation is proposed in [18–19].

Surface roughness was measured by a Qualitest TR100 surface roughness tester. Flank wear and its growth was monitored at regular intervals of length of cut. Digital microscope with maximum magnification of 230× was used to check the wear on flank surfaces as shown in Fig. 1b. Desired cutting speeds were achieved by using different workpiece diameters and rotational speed available in the machine.

3.2. Cutting force and surface roughness models

Experimental matrix and results of cutting force components and surface roughness when turning a work material hardened to 35 and 45 HRC; is shown in Tables 3 and 4, respectively. Regression equations for tangential force (P_1), axial force (P_2) and radial force (P_3) and surface roughness (R_a) were developed based on experimental data. The values of the coefficients involved in the equation were calculated by regression method by using the Design Expert software. Equations developed for three components of cutting force and surface roughness for different work material hardness are given below:

(a) Cutting force components (work material hardness: 35 HRC).

$$P_1 = -373.0294 + 0.5308 * V + 788.3909 * f + 697.2733 * d - 7.2420 * V * f - 1.9860 * V * d + 235 * f * d + 7.5 * 10^{-3} * V^2 + 6659.8597 * f^2 + 0.5986 * d^2 \quad (1)$$

$$P_2 = +375.4951 - 2.9711 * V - 360.2475 * f + 76.6834 * d + 7.9052 * V * f - 0.4 * V * d - 145 * f * d + 3.9878 * 10^{-3} * V^2 - 1528.4596 * f^2 + 66.7154 * d^2 \quad (2)$$

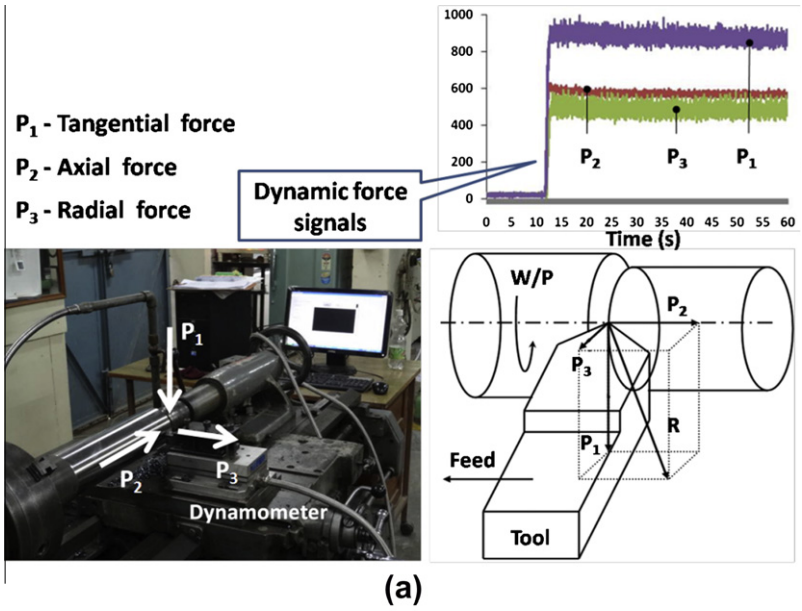

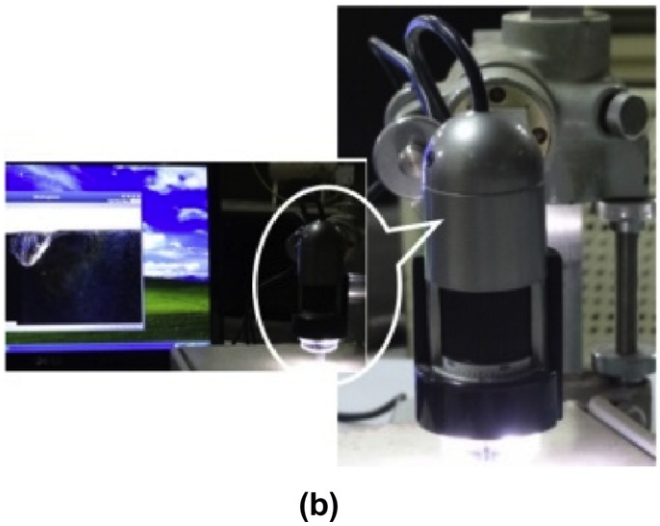

Fig. 1. Measuring instruments (a) cutting force dynamometer and (b) digital microscope.

$$P_3 = +239.6985 - 2.4094 * V + 755.0606 * f + 133.1862 * d - 0.05559 * V * f + 0.2472 * V * d - 585 * f * d + 4.1565 * 10^{-3} * V^2 + 2593.51 * f^2 + 22.9351 * d^2 \quad (3)$$

(b) Cutting force components (work material hardness: 45 HRC).

$$P_1 = -50.5057 - 0.1484 * V + 3270.114 * f + 143.1023 * d - 33.5 * V * f + 1.11 * V * d + 1175 * f * d + 0.01183 * V^2 + 5909.091 * f^2 - 38.9091 * d^2 \quad (4)$$

$$P_2 = +260.483 - 0.86523 * V - 287.159 * f + 113.8068 * d - 6.9 * V * f - 1.39 * V * d + 695 * f * d + 0.01210 * V^2 + 3477.273 * f^2 + 41.2727 * d^2 \quad (5)$$

$$P_3 = 86.3465 - 1.5970 * V + 948.0681 * f + 212.0113 * d - 7.9 * V * f - 1.19 * V * d + 95 * f * d + 0.01518 * V^2 + 2695.4545 * f^2 + 26.9545 * d^2 \quad (6)$$

(c) Surface roughness (work material hardness: 35 HRC).

Table 3
Experimental matrix showing force and surface roughness results (35 HRC).

Cutting speed (V) (m/min)	Feed (f) (mm/rev)	Depth of cut (d) (mm)	Work material hardness: 35 HRC			
			P_1(N)	P_2 (N)	P_3 (N)	R_a (μm)
100	0.2	1.5	841	441	402	6.18
142	0.15	1	403	287	261	5.71
200	0.2	2.5	1031	605	496	6.36
200	0.2	1.5	708	361	344	5.29
142	0.15	2	853	480	403	5.73
265	0.15	2	675	361	365	4.89
265	0.25	1	687	402	312	5.07
200	0.2	0.5	337	257	208	5.03
200	0.3	1.5	938	555	447	6.48
265	0.15	1	461	219	197	4.65
200	0.2	1.5	694	391	331	5.48
200	0.2	1.5	656	383	336	5.39
300	0.2	1.5	670	362	343	5.45
142	0.25	2	1197	553	460	6.81
142	0.25	1	715	377	382	5.76
265	0.25	2	916	532	427	6.48
200	0.2	1.5	708	351	331	5.37
200	0.2	1.5	678	350	316	5.25
200	0.2	1.5	688	376	303	5.53
200	0.1	1.5	562	253	263	4.98

Table 4
Experimental matrix showing force and surface roughness results (45 HRC).

Cutting speed (V) (m/min)	Feed (f) (mm/rev)	Depth of cut (d) (mm)	Work material hardness: 45 HRC			
			P_1(N)	P_2 (N)	P_3 (N)	R_a (μm)
175	0.25	2	1118	557	492	5.48
150	0.3	1.5	1088	592	506	5.81
150	0.2	1.5	830	476	386	4.33
150	0.1	1.5	615	352	314	3.74
125	0.15	2	894	489	433	4.36
150	0.2	1.5	793	432	383	4.53
125	0.25	2	1296	663	559	5.55
150	0.2	1.5	784	430	377	4.14
175	0.25	1	609	421	405	4.48
200	0.2	1.5	759	432	397	4.23
175	0.15	1	492	351	328	3.63
150	0.2	0.5	342	298	256	3.88
150	0.2	1.5	783	431	383	4.26
150	0.2	2.5	1165	659	564	5.13
175	0.15	2	927	457	407	4.38
125	0.15	1	558	353	296	4.24
100	0.2	1.5	885	503	445	4.98
125	0.25	1	799	418	411	4.94
150	0.2	1.5	822	437	377	4.26
150	0.2	1.5	806	417	413	4.37

$$R_a = +12.7937 - 0.03118 * V - 28.8786 * f - 2.8599 * d + 0.0358 * V * f + 2.36 * 10^{-3} * V * d + 11 * f * d + 3.81 * 10^{-5} * V^2 + 32.039 * f^2 + 0.2853 * d^2 \quad (7)$$

(d) Surface roughness (work material hardness: 45 HRC).

$$R_a = +11.3037 - 0.0614 * V - 16.075 * f - 2.3075 * d + 6 * 10^{-3} * V * f + 0.0102 * V * d + 3.7 * f * d + 1.28 * 10^{-4} * V^2 + 49 * f^2 + 0.22 * d^2 \quad (8)$$

3.3. Adequacy of the model

The adequacies of the developed equations were checked by Analysis of Variance (ANOVA) technique. *R*-squared is a coefficient of multiple determinations, which measures variation proportion in the data points. It is always desirable that the correlation coefficient (*R*-square) must range from −1 to +1. The equation is considered to be significant if the value of *R* is very close to +1. *R*-squared adjusted is a measure of the amount of variation about the mean explained by the model. Predicted *R*-squared is a measure of how good the model predicts a response value. The Adjusted and Predicted *R*-squared values should be within about 0.20 of each other, to be in "reasonable agreement." If they are not, there may be a problem with either the data or the model. Adequate precision is a measure of the range in predicted response about its associated error, in other words a signal to noise ratio. Its desired value is 4 or more.

In the present case, the values of *R*-squared are very close to 1; the Adjusted and Predicted R-squared values are in reasonable agreement. Adequate precision values are more than 4; therefore the equations obtained are significant. The model *F*-value obtained for all the equations also implies that the model is significant. ANOVA results for the cutting force components and surface roughness are depicted in Table 5. Percentage contribution of each factor in different responses is discussed in Section 4.1.

3.4. Tool life model

Using ISO 3685-1977(E) as a guide, the tool wear criterion used were when the maximum width of the flank wear land, VB_{max} = 0.2 mm or when the maximum width of the end clearance wear (VC_{max}) or nose wear (NW_{max}) reached 0.2 mm or the occurrence of the catastrophic failure. Experiments were carried out varying cutting speed and feed as per the CCD test matrix with an alpha value of 1.414 (Table 2), using constant depth of cut of 0.8 mm. Experimental matrix and results of tool life test are shown in Tables 6 and 7. In order to consider the effect of depth of cut on tool life, additional seven experiments were performed at various depths of cut. Experimental matrix and results of this tool life test is shown in Table 8.

A modified Taylor tool life equation considering the effect of cutting speed, feed and depth of cut was developed based on experimental data. The tool life (T) results were analyzed using the least error square method. The whole tool life experiments resulted in more equations than unknown coefficients, namely, exponents of V, f, d as 'p', 'q' 'r', respectively, and constant 'c'. As the number of equations was more than the number of unknowns, matrix resulted into over-determined. The unknown coefficients

were determined using Data-Fit software, which uses the following logic for making over-determined matrix into square matrix as described below:

$$VT^p f^q d^r = c,$$

$$p\log T_i + q\log f_i + r\log d_i - \log c = -\log V_i, \forall i \in \begin{Bmatrix} 1---13 & \text{for 35 HRC} \\ 1---12 & \text{for 45 HRC} \end{Bmatrix}.$$

$$[\log T_i \quad \log f_i \quad \log d_i \quad -1] \cdot \begin{Bmatrix} p \\ q \\ r \\ \log c \end{Bmatrix} = \{-\log V_i\},$$

writing as, $A \cdot X = B$,

Then, $X = (A^t \cdot A)^{-1} \cdot (A^t \cdot B)$.

The unknown coefficients are thus calculated. For simplicity, a modified Taylor tool life equation for both the work material is expressed as below.

(a) Tool life model (work material hardness: 35 HRC).

$$T * V^{0.5937} * f^{0.4697} * d^{0.4743} = 423.199 \quad (9)$$

(b) Tool life model (work material hardness: 45 HRC).

$$T * V^{1.548} * f^{0.473} * d^{0.749} = 23135.13 \quad (10)$$

The *R*-squared values of tool life model are 0.9078 (35 HRC) and 0.8826 (45 HRC), respectively, indicates that the developed models can be used to predict the tool life during turning of hardened steel. However, these equations are valid for a flank wear length value lower than 0.2 mm and in the feed range of 0.1–0.3 mm/rev, depth of cut in the range of 0.5–1.5 mm and cutting speed in the range as given in Table 2.

4. Results and discussion

In this section, effect of work material hardness and cutting parameters on performance of coated carbide tool is discussed based on the developed regression equations (as discussed in Sections 3.2 and 3.4). Curves showing the three components of cutting force and tool life are plotted by varying one of the input parameter and keeping the other parameters constant. 3D surface plots for the interaction effects on surface roughness and contribution of cutting parameters in different responses are plotted. Further, a desirability function approach is addressed for simultaneous optimization of performance measures.

4.1. Effect of cutting parameters on force components

Fig. 2a depicts the variation of cutting force components; tangential (P_1), axial (P_2) and radial (P_3); with cutting speed, plotted using feed value of 0.2 mm/rev and depth of cut of 1.5 mm. It can be seen that all the three components of cutting forces are higher for harder work material. The tangential component of cutting force is the largest in magnitude followed by the axial force and radial force. Decrease in tangential component can be seen with the increase in cutting speed. However, in case of softer workpiece, curve remains practically unaltered in cutting speed range of 240–260 m/min. Axial and radial components are also showing similar behavior; initially decrease with the increase in cutting speed, but remains practically unaltered in the higher cutting speed range. However, in case of harder workpiece, these components tend to increase when cutting speed exceeds 160 m/min. This may be because of change in frictional conditions due to increased tool wear at higher cutting speed range.

These research findings are in line with the results obtained by Lima et al. [1], except in their study they have obtained magnitude of radial force higher than that of axial force. However, in the present investigation lower magnitude of radial force resulted from the side cutting edge angle of 75°, which have reduced the contact area where the radial force is applied. Another reason for deviation is due to larger depth of cut (of 1.5 mm) than the tool nose radius (of 0.8 mm). This tool geometry combined with the higher depth of cut causes cutting prominently with the straight section of the side cutting edge along with the tool nose, resulting in higher axial force component than radial component.

Variation of cutting force components with respect to feed and depth of cut are shown in Figs. 2b and c. It can be seen that cutting forces; especially the tangential force vary almost linearly with feed and depth of cut. This is expected also as the magnitude of the tangential force predominantly determined by the cross-section of a cut, which increases with the feed and depth of cut [20]. Depth of cut having the largest contribution; nearly 60–70% followed by feed; nearly 25–30% and cutting speed having little influence; nearly 4–5%, on cutting force components can be seen, from Fig. 3. However, feed having the largest contribution followed by depth of cut and little influence

Table 5
ANOVA results for cutting force components and surface roughness.

Factors	Work material hardness:35 HRC				Work material hardness:45 HRC			
	P_1	P_2	P_3	R_a	P_1	P_2	P_3	R_a
R-squared	0.98	0.98	0.98	0.98	0.99	0.97	0.97	0.97
Adj. *R*-squared	0.97	0.97	0.96	0.96	0.98	0.96	0.95	0.96
Pred. *R*-squared	0.89	0.95	0.92	0.90	0.94	0.91	0.84	0.92
Adeq. precision	33.66	36.36	31.13	23.65	42.73	25.87	22.77	27.07
Model *F*-value	73.54	103.52	66.80	48.35	124.64	52.59	42.3618	53.42

Table 6
Experimental matrix and results for tool life test (35 HRC).

Condition index	Cutting speed (m/min)	Feed (mm/rev)	Tool life (min)	Mode of tool failure
1	265	0.275	27	NW_{max} reached
2	200	0.2	51	VB_{max} reached
3	300	0.2	33	VC_{max} reached
4	142	0.275	42	VB_{max} reached
5	200	0.3	37	VB_{max} reached
6	100	0.2	61	VB_{max} reached
7	200	0.1	55	VB_{max} reached
8	142	0.125	68	Catastrophic failure
9	265	0.125	48	VB_{max} reached

Table 7
Experimental matrix and results for tool life test (45 HRC).

Condition index	Cutting speed (m/min)	Feed (mm/rev)	Tool life (min)	Mode of tool failure
A1	200	0.2	17	NW_{max} reached
A2	150	0.2	35	VB_{max} reached
A3	175	0.125	22	NW_{max} reached
A4	100	0.2	48	VB_{max} reached
A5	125	0.125	40	VB_{max} reached
A6	150	0.1	34	NW_{max} reached
A7	175	0.275	17.5	Catastrophic failure
A8	125	0.275	26	VB_{max} reached
A9	150	0.3	14.5	VB_{max} reached

Table 8
Experimental matrix and results for tool life test for different depth of cut.

Condition index	Cutting speed (m/min)	Feed (mm/rev)	Depth of cut (mm)	Work material hardness (HRC)	Tool life (min)
10	142	0.2	0.5	35	68
11	200	0.2	1.5	35	36
12	265	0.2	1.5	35	19
13	142	0.2	1.5	35	44
A10	142	0.2	0.5	45	39
A11	142	0.2	1.5	45	18
A12	105	0.3	1.5	45	22

by cutting speed was reported in [3]. The reason of discrepancy may be due to the difference in the type of tool holder and multi-layer coated insert used. The another reason may be due to the wider range of depth of cut considered in the present study as against the limited range (0.6–1 mm) used in [3].

Cutting forces observed to be reduced while machining hard work material at higher cutting speed coupled with higher feed or higher depth of cut. Higher temperatures are generated while machining harder material at higher cutting conditions, resulted in reduction of the shear strength of the work material and hence, reduction in the cutting forces. Effect of higher feed and higher depth of cut on axial and radial force components; especially at higher cutting speed can be seen from Fig. 4a and b, respectively. At outer-corner points, feed and depth of cut values (f, d) are plotted. The cutting forces produced are plotted on diagonals of the square. It can be seen that, cutting forces which are higher initially for harder work material at lower feed or at lower depth of cut, have reduced and become nearly equal to that of softer material at higher feed or higher depth of cut.

4.2. Effect of cutting parameters on surface roughness

Figs. 5 and 6 depicts the 3D surface plots of surface roughness for a work material hardened to 35 and 45 HRC, respectively. The interaction effects of cutting parameters on surface roughness can be seen. In surface roughness model (Eq. (7)), terms $V \times f$ and $f \times d$ have appeared as the significant model terms, which have an interaction effects on surface roughness. As seen from Fig. 5a and b, at a lower feed, surface roughness decreases with increase in cutting speed and remains almost unaltered with increase in depth of cut. However, at a higher feed, surface roughness increases sharply with increase in depth of cut. It can be seen that higher feed coupled with higher depth of cut significantly affects the surface roughness. This can be explained in terms of higher cutting forces involved during cutting at higher feed and depth of cut, resulting into more vibrations and hence chatter marks on the machined surface.

However, for harder workpiece, the terms $V \times d$ and $f \times d$ (Eq. (8)) have appeared as the significant model terms, which have an interaction effects on surface roughness. As seen from Fig. 6a and b, at a lower depth of cut, surface roughness decreases with increase in cutting speed and increases with increase in feed. However, at higher depth of cut, surface roughness remains almost unaltered with increase in cutting speed and increases sharply with increase in feed. It can be seen that surface roughness gets affected significantly at higher feed and higher depth of

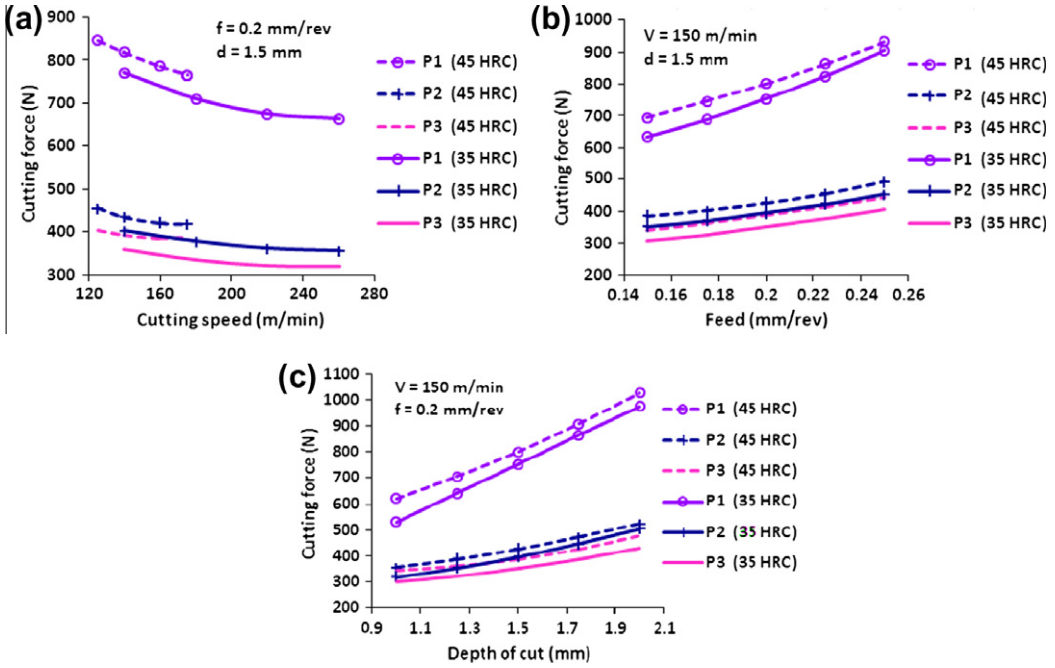

Fig. 2. Effect on cutting force by (a) cutting speed, (b) feed and (c) depth of cut.

cut. However, this effect is observed to be less prominent in case of harder workpiece (Fig. 6b). This may be because of reduction in cutting forces occurred due to softening of the harder material at higher feed and depth of cut, as discussed in Section 4.1.

Percentage contribution of each cutting parameter on surface roughness can be seen from Fig. 3. It can be seen that surface roughness gets affected mostly by feed followed by depth of cut. Lower surface roughness values obtained when turning harder material can be attributed to smooth and continuous chip formed without built-up edge.

4.3. Effect of cutting conditions on tool life

Plots showing the predicted values of tool life (using Eqs. (9) and (10)) along with the experimental values are shown in Fig. 7a and b. It can be seen that, predicted values are in agreement with the experimental values with an average error less than 10%. Histograms showing the predicted tool life with varying one of the input parameters by keeping the other parameters constant are shown in Fig. 8. It can be seen that increase in cutting speed from 100 to 200 m/min causes a decrease in the tool life of about 32% and 65% and the increase in depth of cut from 0.5 to 1.5 mm, causes a decrease of about 35% and 57% when turning 35 and 45 HRC work material, respectively (Fig. 8a and c). However, increase in the feed from 0.1 to 0.3 mm/rev causes a decrease in the tool life of about 40% in case of both the work material (Fig. 8b). It can be seen that, cutting speed followed by depth of cut become the most influencing factors on tool life for harder material. Feed almost have the same effect on tool life irrespective of the hardness of the work material.

Flank wear progression of coated carbide tool during turning at two different levels of hardness of workpiece using cutting speed of 200 m/min, feed value of 0.2 mm/rev and depth of cut of 0.8 mm is shown in Fig. 9. Experimental observations indicate that the wear land on flank face increases with cutting time; generally confined to three distinct regions, namely, initial breakdown, uniform wear rate, and rapid breakdown of the cutting edge. Flank and nose wear, chipping at the nose and clearance face; especially when turning harder material was observed as a dominant wear form and it probably occurred by both abrasive and adhesive wear mechanisms. The tool images at the end of cutting at condition indexes 1 and 2; when turning 35 HRC work material (Table 6), and at condition indexes A1 and A6; when turning 45 HRC work material (Table 7), are shown in Figs. 10a–d, respectively. Flank and clearance face wear and chipping of the coating layers by brittle fracture, which has severely damaged the nose, can be seen.

5. Optimization of cutting conditions

Over the years, many researchers developed algorithms based on classical techniques such as least-squares (LSs) and many others for the domain engineering applications [21,22]. A desirability function approach, presented by Derringer and Suich [23], was employed for simultaneous optimization of response variables; cutting force components (P_1, P_2 and P_3), surface roughness (R_a) and tool life (T). With this approach, each response variable is trans-

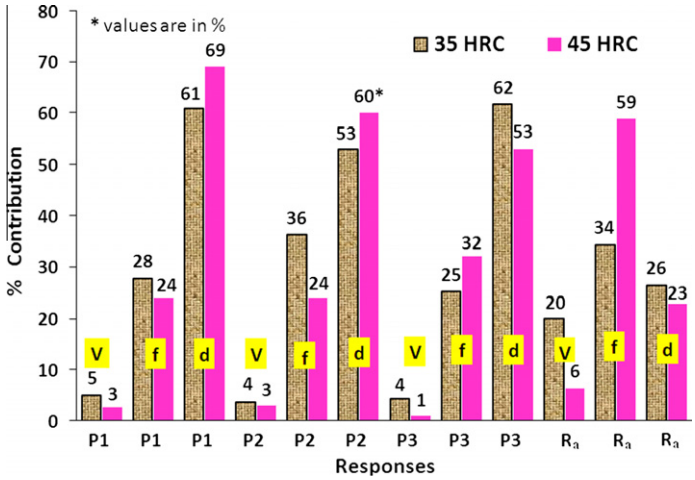

Fig. 3. Percentage contribution of each factor (V, f, and d) in different responses.

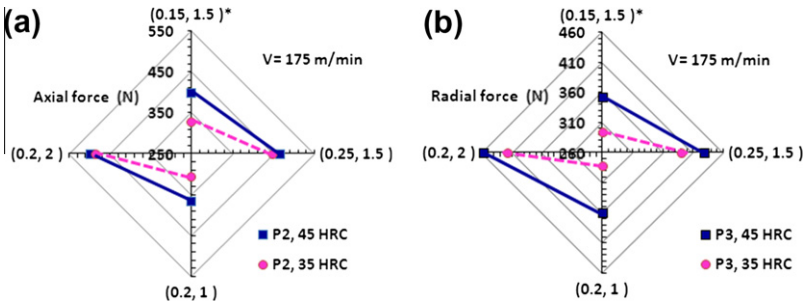

Fig. 4. Effect of cutting parameters on (a) axial force (P_2) and (b) radial force (P_3).

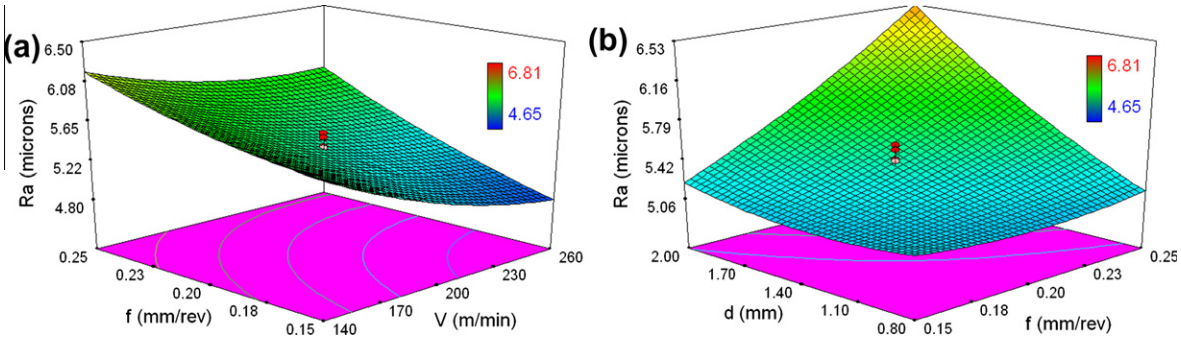

Fig. 5. 3D surface plots for interaction effects for 35 HRC (a) $V \times f$, for d = 1.5 mm and (b) $f \times d$, for V = 200 m/min.

formed into desirability function (D_i). The desirability function is a dimensionless number, which varies between '0' and '1'. '0' indicates the completely undesirable level of response. '1' indicates the completely acceptable level of response. With this approach, optimization of several response variables; (R_i), are converted into optimization of single desirability function; 'D_m'. 'D_m' is the geometric mean of the several responses desirability, which can be obtained using Eq. (11), as given below,

$$D_m = (D_1 * D_2 * D_3 * - - - * D_n)^{1/n} \quad (11)$$

where 'n' is the number of response variables and 'D_i' is the desirability function of each response variable. 'D_m' has to be optimized with respect to process variables. Each response 'R_i' is transformed into each 'D_i' by using one-sided transformation. In one-sided transformation desirability function increases as response function increases (maximization problem) or decreases (minimization problem). One

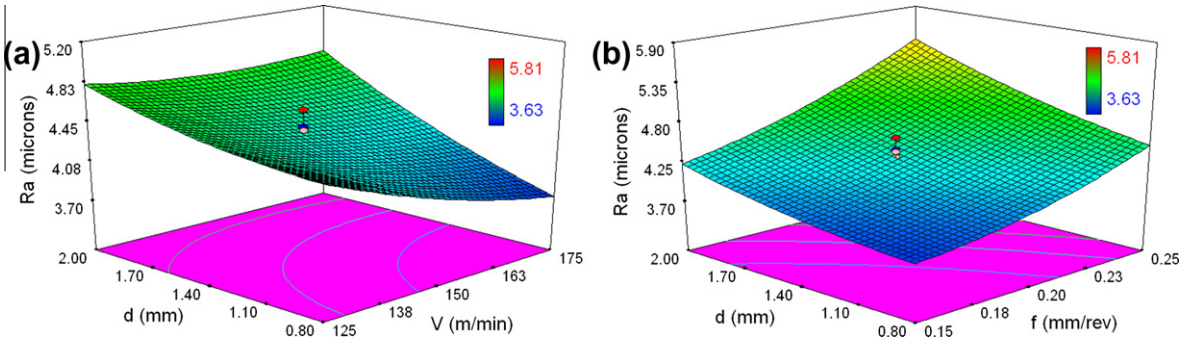

Fig. 6. 3D surface plots for interaction effects for 45 HRC (a) $V \times d$, for $f = 0.2$ mm/rev and (b) $f \times d$, for $V = 150$ m/min.

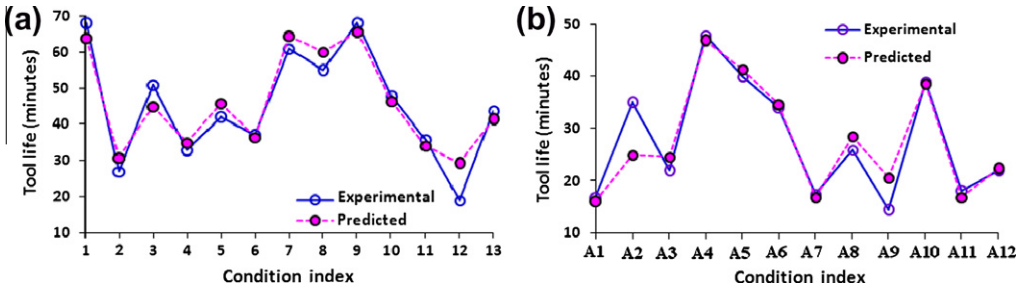

Fig. 7. Comparison between experimental and predicted values for tool life (a) 35 HRC and (b) 45 HRC.

sided transformation in general can be given by the following equation,

$$D_i = \begin{Bmatrix} 0,1 & R_i \leqslant R_{\min} \\ \left[\frac{R_i - R_{\min}}{R_{\max} - R_{\min}}\right], & R_{\min} < R_i < R_{\max} \\ 1,0 & R_i \geqslant R_{\max} \end{Bmatrix} \quad (12)$$

In the present study, the goal was to find the optimum values of process variables (cutting speed, feed and depth of cut) in order to get better tool life, minimum cutting forces (P_1, P_2 and P_3) and minimum surface roughness (R_a), during turning of AISI 4340 steel; hardened to 35 and 45 HRC, respectively. Optimization study was carried out in two different modules; the first module generates a set of solutions which ensures minimum surface roughness and cutting forces. The second module selects a most optimum cutting condition among the solutions generated in module 1, which gives better tool life. Process variables and response functions range are given in Table 9. Minimum and maximum limits of cutting forces and surface roughness are obtained from Tables 3 and 4. The Design Expert software 7.0 was used to find the optimum values

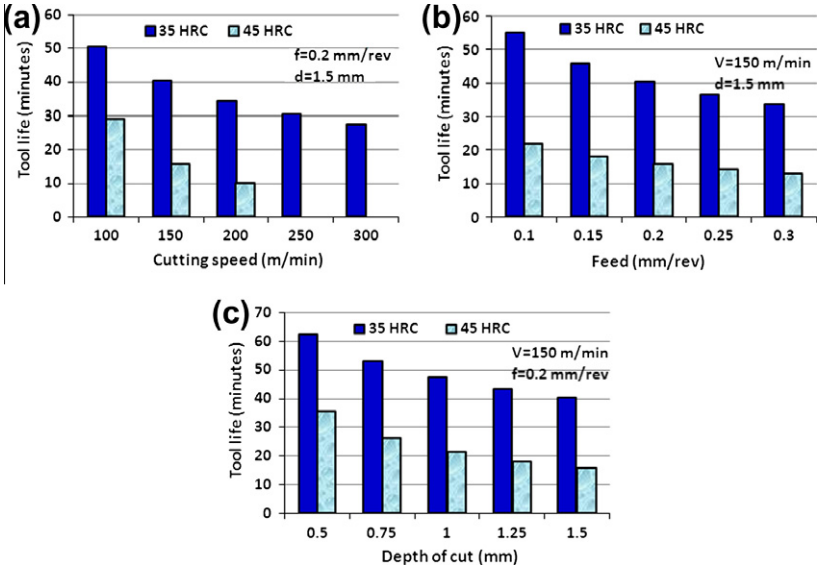

Fig. 8. Effect on tool life by (a) cutting speed, (b) feed and (c) depth of cut.

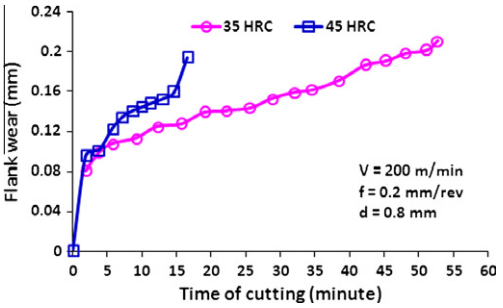

Fig. 9. Flank wear progression when turning a work material hardened to 35 and 45 HRC.

of cutting speed, feed and depth of cut to minimize the tangential, axial, radial force components and surface roughness (module 1). The program calculates 'D_{PSR}' (desirability for cutting force components and surface roughness) for each level of independent parameter and then finds the maximum value of 'D_{PSR}'. Solutions generated for module 1 with their desirability level are shown in Tables 10 and 11 (column 5). Tool life for each obtained solution was calculated using modified Taylor tool life equation (Eqs. (9) and (10)), and shown in column 6.

The second module selects an optimum cutting condition for better tool life. One sided transformation for tool life can be expressed by substituting the minimum and maximum limit of the tool life. Minimum limit was calculated by substituting the higher cutting conditions (V = 300 and 200 m/min for 35 and 45 HRC, respectively, and f = 0.3 mm/rev and d = 1.5 mm), in the developed modified Taylor tool life equation. However, maximum limit of the tool life was selected from column 6 of Tables 10 and 11, respectively. One sided transformation for tool life; 'D_T', for 35 and 45 HRC work material can be expressed as given in Eqs. (13) and (14), as,

$$D_T = \begin{cases} 0, T \leqslant 21 \\ \left[\frac{T-T_{\min}}{T_{\max}-T_{\min}}\right], \quad 21 < T < 40.4 \\ 1, T \geqslant 40.4 \end{cases} \tag{13}$$

$$D_T = \begin{cases} 0, T \leqslant 9 \\ \left[\frac{T-T_{\min}}{T_{\max}-T_{\min}}\right], \quad 9 < T < 25.8 \\ 1, T \geqslant 25.8 \end{cases} \tag{14}$$

For each level of independent parameters, 'D_T' (desirability for tool life) was calculated as shown in column 7 (Tables 10 and 11). Then, a single desirability function 'D_m' (desirability for minimum cutting force, surface roughness and better tool life) was calculated by substituting the 'D_{PSR}' and 'D_T' values in Eq. (11) as shown in column 8. The solution having the highest desirability level ('D_m') is selected as an optimum cutting condition, which is shown in bold face in Tables 10 and 11.

In the present investigation, it is found that, the lower feed value of 0.15 mm/rev, depth of cut of 1 mm and cut-

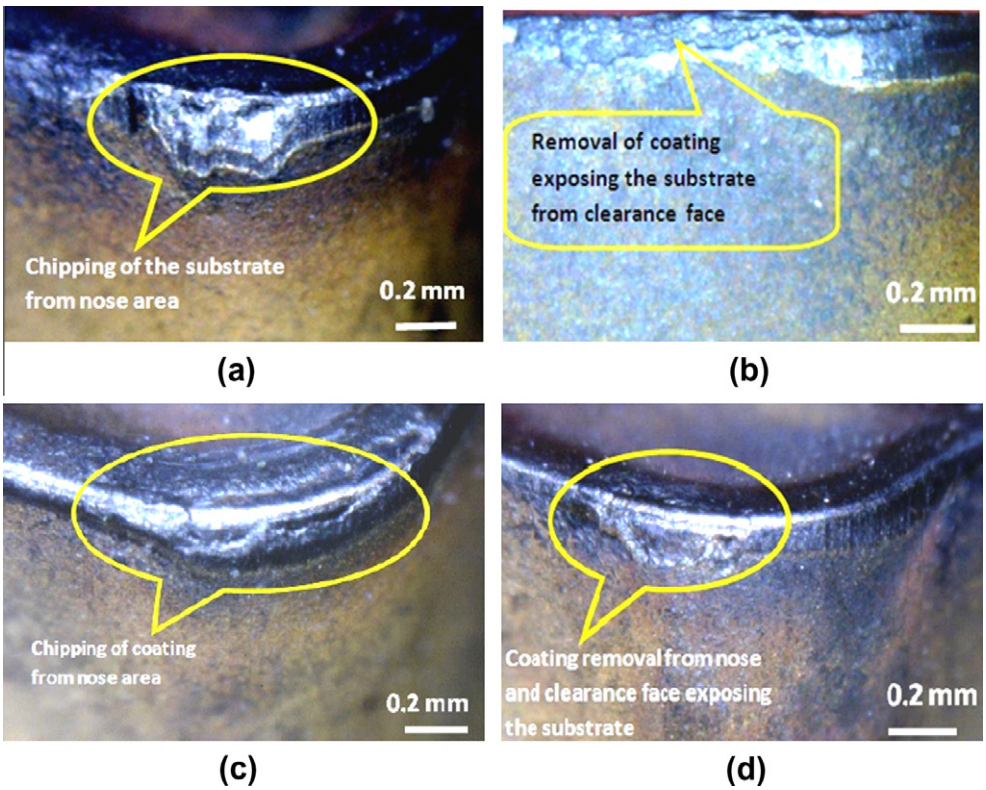

Fig. 10. Images of the tool at the end of tool life at (a) condition index 1, (b) condition index 2, (c) condition index A1, and (d) condition index A6.

Table 9
Constraints for optimization of cutting parameters.

Parameters	Goal	35 HRC		45 HRC	
		Minimum limit	Maximum limit	Minimum limit	Maximum limit
Cutting speed, V (m/min)	Is in range	142	265	125	175
Feed, f (mm/rev)	Is in range	0.15	0.25	0.15	0.25
Depth of cut, d (mm)	Is in range	1	2	1	2
Tangential force (P_1)	Minimize	337	1197	492	1296
Axial force (P_2)	Minimize	219	605	298	663
Radial force (P_3)	Minimize	197	496	256	564
Surface roughness (R_a)	Minimize	4.65	6.81	3.63	5.81

Table 10
Optimized cutting parameters for work material hardened to 35 HRC.

Sr. no.	V (m/min)	f (mm/rev)	d (mm)	1 R_a (μm)	2 P_1 (N)	3 P_2 (N)	4 P_3 (N)	5 Desirability D_{PSR}	6 T (minute)	7 Desirability D_T	8 Desirability D_m
1	258	0.15	1	4.75	472	218	196	0.95	38.2	0.89	0.92
2	257	0.15	1	4.75	471	219	196	0.95	38.3	0.89	0.92
3	256	0.15	1	4.76	470	219	196	0.95	38.3	0.89	0.92
4	255	0.15	1	4.76	468	219	197	0.95	38.4	0.90	0.92
5	261	0.15	1	4.74	477	218	196	0.95	37.9	0.87	0.91
6	260	0.15	1	4.74	476	219	197	0.95	38.0	0.88	0.91
7	265	0.15	1	4.73	482	218	197	0.95	37.6	0.85	0.90
8	263	0.15	1	4.74	480	220	198	0.94	37.8	0.86	0.90
9	259	0.15	1	4.75	476	221	198	0.94	38.0	0.88	0.91
10	243	0.15	1	4.82	454	221	198	0.94	39.6	0.96	0.95
11	**235**	**0.15**	**1**	**4.86**	**445**	**224**	**199**	**0.94**	**40.4**	**1.00**	**0.97**
12	242	0.15	1	4.82	453	222	198	0.94	39.7	0.96	0.95
13	264	0.15	1.03	4.73	486	220	201	0.94	37.2	0.83	0.89
14	261	0.15	1.03	4.74	484	221	201	0.94	37.4	0.84	0.89
15	239	0.15	1.17	4.83	493	240	224	0.90	37.1	0.83	0.86
16	214	0.17	1	4.99	452	253	220	0.88	40.2	0.99	0.94
17	265	0.15	1.27	4.76	542	250	243	0.87	33.5	0.65	0.75

Optimized cutting parameters are shown in bold.

Table 11
Optimized cutting parameters for work material hardened to 45 HRC.

Sr. no.	V (m/min)	f (mm/rev)	d (mm)	1 R_a (μm)	2 P_1 (N)	3 P_2 (N)	4 P_3 (N)	5 Desirability D_{PSR}	6 T (minute)	7 Desirability D_T	8 Desirability D_m
1	159	0.15	1	3.69	507	338	295	0.89	22.2	0.78	0.84
2	160	0.15	1	3.68	506	339	296	0.89	21.9	0.77	0.83
3	158	0.15	1	3.70	507	338	294	0.89	22.3	0.79	0.84
4	157	0.15	1	3.71	507	337	293	0.89	22.6	0.81	0.85
5	162	0.15	1	3.66	506	340	298	0.89	21.5	0.74	0.81
6	151	0.15	1	3.77	510	334	289	0.89	23.9	0.89	0.89
7	149	0.15	1	3.80	511	334	288	0.89	24.5	0.92	0.90
8	170	0.16	1	3.63	509	347	309	0.88	19.5	0.62	0.74
9	**144**	**0.15**	**1**	**3.86**	**514**	**332**	**285**	**0.88**	**25.8**	**1.00**	**0.94**
10	161	0.16	1	3.71	514	343	303	0.88	21.1	0.72	0.79
11	175	0.15	1	3.57	505	350	312	0.87	19.2	0.61	0.73
12	175	0.17	1	3.65	514	356	322	0.86	18.0	0.54	0.68
13	171	0.15	1.08	3.63	538	352	313	0.86	18.7	0.58	0.71
14	144	0.16	1	3.92	534	339	296	0.86	25.1	0.96	0.90
15	175	0.15	1.24	3.70	609	366	331	0.81	16.3	0.43	0.59
16	175	0.15	1.3	3.73	633	371	336	0.79	15.7	0.40	0.56

Optimized cutting parameters are shown in bold.

ting speed of 235 and 144 m/min, while turning 35 and 45 HRC work material, respectively, are the optimum cutting parameters results in minimum cutting forces, surface roughness and better tool life. The results obtained are found to be comparable to other studies. Sahoo et al. [7] observed better performance of multi-layer TiN coated carbide inserts at cutting speed of 150 m/min and at lower feed and depth of cut while turning 48 HRC steel. Asilturk et al. [2] found cutting speed of 120 m/min, feed of 0.18 mm/rev and depth of cut of 0.4 mm as optimized parameters for minimum surface roughness while turning AISI 4140 steel hardened to 51 HRC. However, with CBN

tools cutting speed of 189 m/min, feed and depth of cut values of 0.08 mm/rev and 0.15 mm resulted in optimum cutting parameters during turning of 42 HRC hot work steel [10].

6. Conclusions

The machining performance of CVD coated multi-layer TiCN/Al_2O_3/TiN carbide tool was assessed during turning of hardened AISI 4340 alloy steel at different levels of hardness. Highly significant parameters were determined by performing an Analysis of Variance (ANOVA). A modified Taylor tool life equation was developed considering the effect of cuttting parameters. The correlation coefficients found close to 0.9, shows that the developed models are reliable and could be used effectively for predicting the responses for the given tool and work material pair and within the domain of the cutting parameters.

Experimental observations indicate that all the three components of cutting forces are higher for harder work material. However, they are observed to be reduced and become nearly equal to that of softer material at higher cutting speed when coupled with higher feed and higher depth of cut. Cutting forces get affected mostly by depth of cut (nearly 60–70% contribution) followed by feed (nearly 25–30% contribution). Surface roughness gets affected significantly at higher feed and depth of cut. However, this effect was observed to be more prominent in case of softer workpiece. Cutting speed followed by depth of cut was found to be the most influencing factors on tool life, especially when turning harder workpiece. Flank and nose wear, chipping of the coating layers from the nose and clearance face of the tool were observed as a dominant wear form; probably occurred by both abrasive and adhesive wear mechanisms. In the present investigation, it is found that, feed value of 0.15 mm/rev, depth of cut of 1 mm and cutting speed of 235 (35 HRC) and 144 m/min (45 HRC) are the optimum cutting parameters for minimum cutting forces, surface roughness and better tool life.

References

[1] J.G. de Lima, R.F. de Avila, A.M. Abrao, Turning of hardened AISI 4340 steel using coated carbide inserts, Proceedings of the IMechE, Part B: Journal of Engineering Manufacture 221 (2007) 1359–1366.
[2] I. Asilturk, H. Akkus, Determining the effect of cutting parameters on surface roughness in hard turning using the Taguchi method, Measurement 44 (2011) 1697–1704.
[3] R. Suresh, S. Basavarajappa, G.L. Samuel, Some studies on hard turning of AISI 4340 steel using multilayer coated carbide tool, Measurement 45 (2012) 1872–1884.
[4] R. Suresh, S. Basavarajappa, V.N. Gaitonde, G.L. Samuel, Machinability investigations on hardened AISI 4340 steel using coated carbide insert, International Journal of Refractory Metals and Hard Materials 33 (2012) 75–86.
[5] S. Yusuf, A.R. Motorcu, Surface roughness model for machining mild steel with coated carbide tool, Materials and Design 26 (2005) 321–326.
[6] M.Y. Noordin, V.C. Venkatesh, S. Sharif, S. Elting, A. Abdullah, Application of response surface methodology in describing the performance of coated carbide tools when turning AISI 1045 steel, Journal of Materials Processing Technology 145 (2004) 46–58.
[7] A.K. Sahoo, B. Sahoo, Experimental investigations on machinability aspects in finish hard turning of AISI 4340 steel using uncoated and multilayer coated carbide inserts, Measurement 45 (2012) 2153–2165.
[8] A.K. Sahoo, B. Sahoo, Surface roughness model and parametric optimization in finish turning using coated carbide insert: response surface methodology and Taguchi approach, International Journal of Industrial Engineering Computations 2 (2011) 819–830.
[9] M.C. Cakir, C. Ensarioglu, I. Demirayak, Mathematical modeling of surface roughness for evaluating the effects of cutting parameters and coating material, Journal of Materials Processing Technology 209 (2009) 102–109.
[10] H. Aouici, M.A. Yallese, K. Chaoui, T. Mabrouki, J. Rigal, Analysis of surface roughness and cutting force components in hard turning with CBN tool: prediction model and cutting conditions optimization, Measurement 45 (2012) 344–353.
[11] J.G. Lima, R.F. Ávila, A.M. Abrao, M. Faustino, J.P. Davim, Hard turning: AISI 4340 high strength alloy steel and AISI D2 cold work tool steel, Journal of Materials Processing Technology 169 (3) (2005) 388–395.
[12] T. Ozel, T.K. Hsu, E. Zeren, Effects of cutting edge geometry, workpiece hardness, feed rate and cutting speed on surface roughness and forces in finish turning of hardened AISI H13 steel, International Journal of Advanced Manufacturing Technology 25 (2005) 262–269.
[13] M.A. Federico, T. Coelho Reginaldo, C. Brandao Lincoln, Turning hardened steel using coated carbide at high cutting speeds, Journal of the Brazilian Society of Mechanical Sciences and Engineering 30 (2) (2008) 104–109.
[14] N. Mandal, B. Doloi, B. Mondal, R. Das, Optimization of flank wear using Zirconia Toughened Alumina (ZTA) cutting tool: Taguchi method and regression analysis, Measurement 44 (2011) 2149–2155.
[15] S. Neseli, S. Yaldiz, E. Turkes, Optimization of tool geometry parameters for turning operations based on the response surface methodology, Measurement 44 (2011) 580–587.
[16] Kennametal, KC 9110 and KC9125 Technical Manual, Latrobe, 2001
[17] W.G. Cochran, G.M. Cox, Experimental Designs, John Wiley and Sons Inc., New York, 1957.
[18] D.N. Vizireanu, A fast, simple and accurate time-varying frequency estimation method for single-phase electric power systems, Measurement 45 (2012) 1331–1333.
[19] D.N. Vizireanu, R.O. Preda, Is "five-point" estimation better than "three-point" estimation?, Measurement 46 (2012) 840–842
[20] S.E. Oraby, D.R. Hayhurst, Development of models for tool wear force relationships in metal cutting, International Journal of Machine Tools and Manufacture 33 (2) (1991) 125–138.
[21] D.N. Vizireanu, S.V. Halunga, Simple, fast and accurate eight points amplitude estimation method of sinusoidal signals for DSP based instrumentation, Journal of Instrumentation 7 (4) (2012).
[22] D.N. Vizireanu, S.V. Halunga, Analytical formula for three points sinusoidal signals amplitude estimation errors, International Journal of Electronics 99 (1) (2012) 149–151.
[23] G. Derringer, R. Suich, Simultaneous optimization of several response variables, Journal of Quality Technology 12 (1980) 214–219.